

LETTER TO THE EDITOR

Chemical similarities between Galactic bulge and local thick disk red giant stars

J. Meléndez^{1,2}, M. Asplund³, A. Alves-Brito⁴, K. Cunha^{5,6}, B. Barbuy⁴, M.S. Bessell², C. Chiappini^{7,8}, K.C. Freeman², I. Ramírez⁹, V.V. Smith⁵, and D. Yong²

¹ Centro de Astrofísica da Universidade do Porto, Rua das Estrelas, 4150-762 Porto, Portugal

² Research School of Astronomy and Astrophysics, The Australian National University, Cotter Road, Weston, ACT 2611, Australia

³ Max Planck Institute for Astrophysics, Postfach 1317, 85741 Garching, Germany

⁴ Universidade de São Paulo, IAG, Rua do Matão 1226, Cidade Universitária, São Paulo 05508-900, Brazil

⁵ National Optical Astronomy Observatory, Casilla 603, La Serena, Chile

⁶ On leave from Observatório Nacional, Rio de Janeiro, Brazil

⁷ Geneva Observatory, Ch. des Maillettes 51, 1290 Sauverny, Switzerland

⁸ OAT/INAF, Via Tiepolo 11, Trieste 34131, Italy

⁹ McDonald Observatory and Department of Astronomy, University of Texas, RLM 15.306, Austin, TX 78712-1083, USA

Received: January 15, 2008; accepted: April 18, 2008

ABSTRACT

Context. The evolution of the Milky Way bulge and its relationship with the other Galactic populations is still poorly understood. The bulge has been suggested to be either a merger-driven classical bulge or the product of a dynamical instability of the inner disk.

Aims. To probe the star formation history, the initial mass function and stellar nucleosynthesis of the bulge, we performed an elemental abundance analysis of bulge red giant stars. We also completed an identical study of local thin disk, thick disk and halo giants to establish the chemical differences and similarities between the various populations.

Methods. High-resolution infrared spectra of 19 bulge giants and 49 comparison giants in the solar neighborhood were acquired with Gemini/Phoenix. All stars have similar stellar parameters but cover a broad range in metallicity. A standard 1D local thermodynamic equilibrium analysis yielded the abundances of C, N, O and Fe. A homogeneous and differential analysis of the bulge, halo, thin disk and thick disk stars ensured that systematic errors were minimized.

Results. We confirm the well-established differences for [O/Fe] (at a given metallicity) between the local thin and thick disks. For the elements investigated, we find no chemical distinction between the bulge and the local thick disk, which is in contrast to previous studies relying on literature values for disk dwarf stars in the solar neighborhood.

Conclusions. Our findings suggest that the bulge and local thick disk experienced similar, but not necessarily shared, chemical evolution histories. We argue that their formation timescales, star formation rates and initial mass functions were similar.

Key words. Stars: abundances – Galaxy: abundances – Galaxy: bulge – Galaxy: disk – Galaxy: evolution

1. Introduction

Despite its prominent role in the formation and evolution of the Galaxy, the bulge is the least well-understood stellar population in the Milky Way. Two main formation scenarios have been proposed to explain bulges of spiral galaxies (see Kormendy & Kennicutt 2004, for a review). In classical bulges, most stars are formed during an early phase of intensive star formation following collapse of the proto-galaxy and subsequent mergers, as predicted in a cold dark matter cosmology. Boxy or peanut-shaped bulges develop through dynamical instability of an already established inner disk. The nature of the Galactic bulge is still unknown since its generally old and metal-rich stellar population (e.g. Zoccali et al. 2006; Fulbright et al. 2006) is consistent with a classical bulge while its boxy shape is indicative of formation by dynamical instability.

Compared to the other Galactic populations, our understanding of the chemical properties of the bulge and its evolution with time is still sketchy due to the large distance and high visual extinction. Following pioneering work on 4-m-class telescopes (e.g. McWilliam & Rich 1994), the situation

has, however, improved based on observations with 8-10 m telescopes (e.g. Meléndez et al. 2003; Rich & Origlia 2005; Zoccali et al. 2006; Fulbright et al. 2006, 2007; Cunha & Smith 2006; Lecureur et al. 2007). High-resolution multi-object and infrared (IR) spectrographs have also aided the cause, such that the number of red giants in the bulge with detailed abundance information based on high-resolution spectroscopy now exceeds 100.

Of particular interest are the abundances of α -elements (such as O and Mg) as a function of metallicity, since they provide crucial information about the star formation history and initial mass function (Tinsley 1980; Ballero et al. 2007). In regions of rapid star formation rates – as expected for the Galactic bulge – higher metallicities are reached before the contributions from thermonuclear supernovae (SNe Ia) are reflected in the abundance ratios. The α -element abundances should then remain elevated compared to those parts of the Galaxy experiencing a more modest star formation rate. A tell-tale signature is therefore $[\alpha/\text{Fe}] > 0.0$ at high metallicities ($[\text{Fe}/\text{H}] \approx 0$) as a result of nucleosynthesis in core collapse supernovae (SNe II). A conclusion of most bulge studies is that indeed the α -elements seem

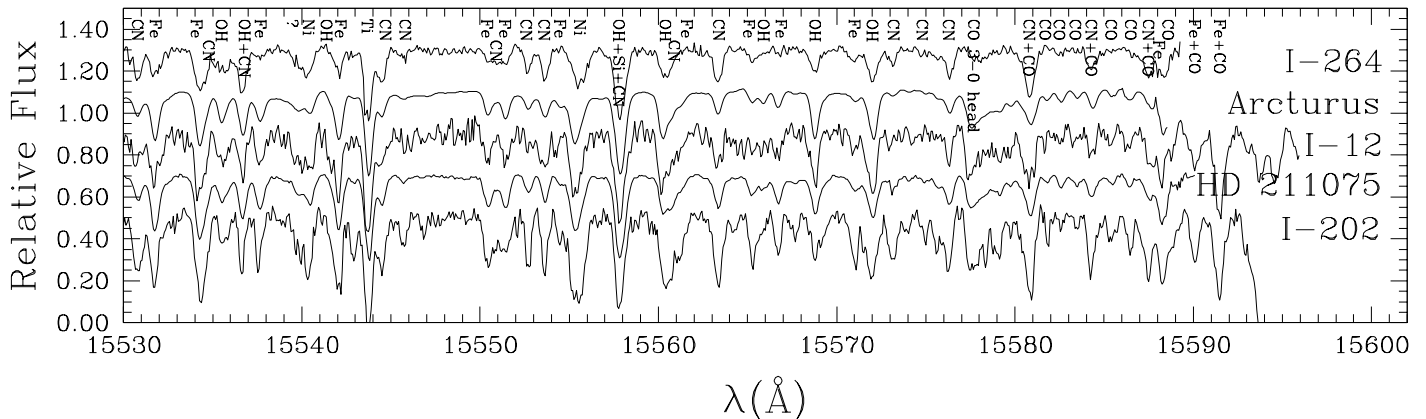


Fig. 1. Observed Phoenix spectra of selected bulge giants as well as thick (Arcturus = HD124897) and thin (HD211075) disk stars.

to be overabundant relative to both the thin and the thick disks in the solar neighborhood, implying a short formation timescale of the bulge (Fulbright et al. 2007; Lecureur et al. 2007).

In this Letter we revisit the issue of the chemical differences between the bulge and the thin/thick disks based on Gemini/Phoenix high-resolution IR spectra of 19 K giants in Baade’s window as well as a sample of nearby thin and thick disk giants. The unique aspect of our study is that we conduct a homogeneous differential analysis of stars with similar stellar parameters to minimize systematic errors. The novel result of our careful analysis is that we find no significant abundance differences for the elements studied (C, N and O) between the bulge and the local thick-disk stars.

2. Observations and abundance analysis

High-resolution ($R \equiv \lambda/\Delta\lambda = 50,000$) IR spectra of 19 K giants in the Baade’s window of the bulge were taken with the Phoenix spectrograph (Hinkle et al. 2003) on the 8 m Gemini-South telescope. The Phoenix spectra of five of these bulge giants were previously analyzed by Cunha & Smith (2006). Importantly, comparison K giants of the thin disk (24 stars), thick disk (21 stars) and halo (4 stars) in the solar neighborhood were observed using the same instrument on Gemini-South as well as the 2.1 m and 4 m Kitt Peak telescopes. The stars were selected to cover the metallicity range $-1.5 \leq [\text{Fe}/\text{H}] \leq +0.5$. The assignment of population membership to the comparison sample was based on UVW velocities (Bensby et al. 2004; Reddy et al. 2006). All IR spectra were obtained using the same instrumental setup centered on $1.5555 \mu\text{m}$ (Fig. 1).

We also acquired high-resolution ($R = 60,000$) optical spectra to check the derived stellar parameters employing Fe I and Fe II lines. The disk and halo stars were observed using the MIKE spectrograph on the Clay 6.5 m Magellan telescope and the 2dcoudé spectrograph on the 2.7 m Harlan J. Smith telescope at McDonald Observatory. For the bulge stars, we rely on the equivalent widths measured by Fulbright et al. (2006, 2007) using the HIRES spectrograph on the Keck-I 10 m telescope. Our observations were acquired between September 1999 and October 2007.

Both the optical and infrared spectra were reduced homogeneously with IRAF; we refer the reader to Meléndez et al. (2003), Yong et al. (2006) and Meléndez & Ramírez (2007) for details on the data reduction of Phoenix, MIKE, and 2dcoude

spectra, respectively. The signal-to-noise ratio (S/N) of the reduced spectra ranges from $S/N \approx 100$ per spectral resolution element, for the IR spectra of the bulge giants, to several hundreds per pixel, for both the optical and IR spectra of the bright disk and halo K giants.

Photometric temperatures were obtained using optical and infrared colors and the infrared flux method T_{eff} -scale of Ramírez & Meléndez (2005). Reddening for the bulge stars was estimated from extinction maps (Stanek 1996) while for the comparison samples both extinction maps and Na I D ISM absorption lines were adopted (Meléndez et al. 2006). The stellar surface gravities were derived from improved Hipparcos parallaxes (van Leeuwen 2007) using bolometric corrections from Alonso et al. (1999) for the relatively nearby disk and halo stars and assuming a distance of 8 kpc for the bulge giants. In addition, Yonsei-Yale (Demarque et al. 2004) and Padova isochrones (da Silva et al. 2006) were employed to determine evolutionary gravities. Tests of the ionization and excitation balances of Fe I and Fe II lines revealed that the photometric stellar parameters of only six stars required significant adjustments; given the remaining uncertainties in both the photometric and spectroscopic parameters the overall agreement for the remaining stars is encouraging. The adopted stellar parameters are given in Table 1. We estimate that our stellar parameters have typical uncertainties of $\Delta T_{\text{eff}} \approx \pm 75 \text{ K}$, $\Delta \log g \approx \pm 0.3$ and $\Delta v_t \approx 0.2 \text{ km s}^{-1}$, which translates into abundance errors for Fe, C, N and O of 0.03, 0.11, 0.11 and 0.14 dex, respectively, when the errors are added in quadrature; the errors in $[\text{X}/\text{Fe}]$ are almost identical. As discussed below, these uncertainties are probably too conservative; an uncertainty in $[\text{O}/\text{Fe}]$ of 0.10 dex was adopted.

The Phoenix spectral window contains several useful lines for abundance purposes. The stellar C, N, O and Fe abundances were obtained from spectrum synthesis of a number of CO, CN, OH and Fe I lines using MOOG (Snedden 1973); it is important to be able to derive the C, N and O abundances consistently for each star given the interdependencies in the respective molecular balance and corresponding line strengths. The same transition probabilities for the atoms and molecules were applied to both the bulge and comparison samples (Meléndez et al. 2003). In the present work, we employed both Kurucz models with convective overshooting (Castelli et al. 1997) and specially calculated MARCS (Gustafsson et al. 2003) 1D hydrostatic model atmospheres. For the MARCS models, both α -enhanced ($[\alpha/\text{Fe}] = +0.2$ and $+0.4$) and scaled-solar abundances models were con-

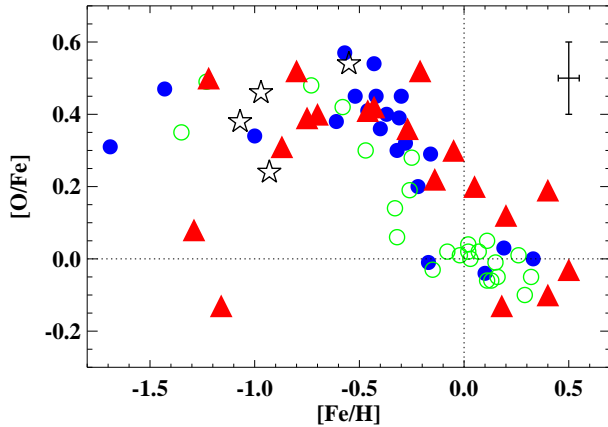


Fig. 2. The derived $[O/Fe]$ ratios, as a function of $[Fe/H]$, for the bulge (red triangles), thick disk (blue solid circles), thin disk (open green circles) and halo giants (stars). A typical error bar is shown. Note the similarities between the bulge and thick disk trends for $[Fe/H] < -0.2$.

structured; for the Kurucz’ models, adjustments of $[Fe/H]$ were applied to simulate the effects of α -enhancement on the model atmospheres: $\Delta[Fe/H] = \log(0.64 \times 10^{[\alpha/Fe]} + 0.36)$ (Salaris et al. 1993). Our final results are based on the MARCS models with appropriate compositions. The effects of failing to account for the variations in $[\alpha/Fe]$ can be substantial: a difference of $[\alpha/Fe] = +0.2$ in the model atmosphere corresponds to a change of $\approx +0.1$ dex in the derived $[O/Fe]$. Otherwise, the agreement between MARCS and Kurucz models is very good: the mean differences for $[Fe/H]$, $[C/Fe]$, $[N/Fe]$ and $[O/Fe]$ between MARCS and Kurucz models are only $+0.01$, $+0.01$, $+0.02$ and $+0.04$ dex, respectively. The corresponding solar abundances for the MARCS suite of models are $\log \epsilon_C = 8.42$, $\log \epsilon_N = 7.82$, $\log \epsilon_O = 8.72$ and $\log \epsilon_{Fe} = 7.48$, similar to the 3D-based values provided by Asplund et al. (2005). For the bulge stars in common, the differences in $[O/Fe]$ between us and Fulbright et al. (2007) is $+0.03 \pm 0.13$ dex.

While no predictions of 3D hydrodynamical models are available for precisely our parameter space of interest (Asplund 2005), we note that, according to simulations of slightly less evolved red giants, the 3D abundance corrections for the species considered herein are expected to be modest: $|\Delta \log \epsilon| \leq 0.1$ dex at $[Fe/H] \geq 0$, although slightly larger at the lowest metallicities of our targets (Collet et al. 2007). Given the similarity in parameters between the bulge and disk giants, the *relative* abundance ratio differences will be significantly smaller.

3. Results

Our results in terms of $[O/Fe]$ are shown in Fig. 2. One concern is whether CNO-cycled material has been dredged-up to the surface in our giants. It is clear that many of the stars’ atmospheres contain CN-cycled gas. As demonstrated in Fig. 3, however, the $[C+N/Fe]$ ratio remains roughly constant at solar values as a function of metallicity for both the bulge and disk giants, which implies that intrinsic CNO-cycled rest-products have not been brought up to the surface. We therefore believe that the measured O abundances are indeed a proper reflection of the pristine contents the stars were born with. We note that Fulbright et al. (2007) argued that the two O-deficient stars (I-264 and IV-203)

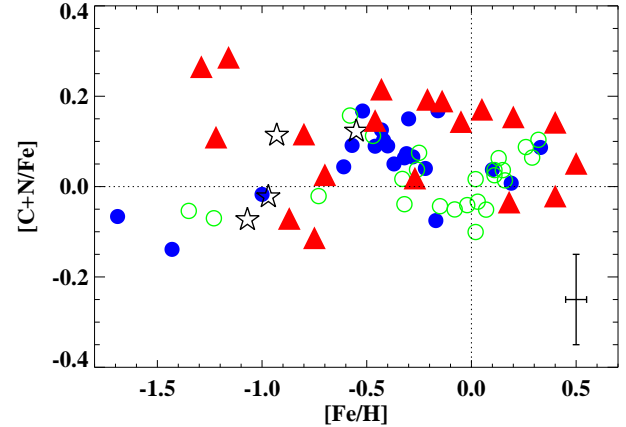


Fig. 3. The derived $[C+N/Fe]$ ratios as a function of $[Fe/H]$ for the bulge (red triangles), thick disk (blue solid circles), thin disk (open green circles) and halo giants (stars). A typical error bar is shown.

at $[Fe/H] \approx -1.2$ have experienced envelope H-burning reminiscent of that believed to be responsible for the O-Na correlations in globular clusters based on the stars’ high Na and Al abundances. It is then surprising that their $[C+N/Fe]$ ratios are normal or only marginally higher as O-depletion in globular cluster stars is associated with increased $[N/Fe]$ ratios due to CNO-cycling (Gratton et al. 2004, and references therein). In any case, we believe that the O abundances of these two stars do not reflect the typical bulge composition.

In agreement with previous findings (Zoccali et al. 2006; Fulbright et al. 2007; Lecureur et al. 2007), the bulge $[O/Fe]$ trend goes from typical halo values to roughly solar or below at $[Fe/H] > 0$. The break in $[O/Fe]$ at $[Fe/H] \approx -0.3$ implies that both SNe II and SNe Ia have contributed and therefore that the formation of the bulge proceeded over several 100 Myr. The plateau in $[O/Fe]$ for the bulge extends to higher metallicities than for the thin disk, implying a higher star formation rate. Furthermore, we confirm the by now well-established chemical distinctions of the Galactic thin and thick disks locally, in the sense that for a given $[Fe/H]$ the latter is more over-abundant in α -elements (Bensby et al. 2004; Reddy et al. 2006). We also seem to detect a similar knee in $[O/Fe]$ for the local thick disk as advocated by Bensby et al. (2004), although this is based on only a handful of stars. The existence of this SNe Ia signature has been questioned by other studies of thick-disk stars (Reddy et al. 2006; Ramírez et al. 2007). The interpretation largely hinges on whether or not the kinematically selected local thick-disk stars at $[Fe/H] \geq -0.2$ truly belong to this population or are just part of the high-velocity tail of the thin disk. As also seen from the four such thick-disk stars included in our sample, there is no chemical differentiation at these metallicities between the thin and thick disk, if indeed the thick disk extends to these high $[Fe/H]$. Our limited number of thick-disk stars is insufficient to draw firm conclusions to these questions. Likewise, the four thin-disk stars with $[Fe/H] < -0.5$ may belong to the thick disk since our classification assumes a metallicity-independent thick/thin disk stellar fraction of 10% (Bensby et al. 2004).

The most surprising inference of our study comes from a comparison of our bulge and local thick-disk samples. In contrast to previous works on the topic (Zoccali et al. 2006; Fulbright et al. 2007; Lecureur et al. 2007), we find that the two

populations are indistinguishable in their abundance patterns for the elements considered (C, N and O) up to $[\text{Fe}/\text{H}] = -0.2$, i.e. to the metallicity range where the thick disk is unambiguously identified. A linear fit to the bulge data is $[\text{O}/\text{Fe}] = 0.41 - 0.02 \times [\text{Fe}/\text{H}]$ while for the thick disk it is $[\text{O}/\text{Fe}] = 0.39 - 0.01 \times [\text{Fe}/\text{H}]$, both with a scatter of $\sigma = 0.09$ dex; the mean difference between the bulge fit and the thick disk data is 0.03 ± 0.09 dex. The comparison implies that the real abundance errors probably do not exceed 0.10 dex rather than the higher estimates given in Sect. 2. The metallicity of the bulge extends to significantly higher $[\text{Fe}/\text{H}]$ than that, which, as explained above, remains to be convincingly demonstrated for the thick disk. Rather than having had a significantly higher star formation rate as normally argued, the conclusion is thus that the bulge did not differ noticeably from the local thick disk in this respect. Furthermore, our observations suggest that the initial mass function for the two populations were similar. The nearly identical $[\text{O}/\text{Fe}]$ trends do not necessarily imply a causal relationship between the bulge and local thick disk. Such a relationship has been proposed for other spiral galaxies (e.g. van der Kruit & Searle 1981) and remains an intriguing possibility based on our observations.

In the classical bulge scenario one does not expect any direct relationship between the bulge and either of the disk populations. Since the thin disk had a long formation timescale and experienced a smaller star formation rate, it is unsurprising that $[\text{O}/\text{Fe}]$ differs between the solar neighborhood thin disk and the bulge. If both the bulge and the thick disk formed on short timescales as well as had similar initial mass function and star formation histories, the abundance pattern would be similar even if the two populations lack a physical connection. In the disk instability formation model for the Galactic bulge, the bulge stellar population consists largely of stars from the inner disk that have been heated dynamically through the instabilities associated with bar formation and buckling. According to N-body simulations, the bar and consequently the bulge appears only after a few Gyr, when the thick disk was already in place according to the observed stellar ages of ≥ 9 Gyr (Bensby et al. 2007). However, it is important to distinguish between the ages of the stars and the ages of the structures that they inhabit. The stars of the bulge and thick disk appear to be very old. If the bulge and thick disk both formed dynamically (e.g. via instabilities or minor merger heating of the early thin disk), then the bulge and thick-disk stars may well be significantly older than the bulge and thick-disk structures, and the bulge-thick disk similarities which we have uncovered would then not be surprising. The differences between the bulge and our thin-disk stars do not support a causal link between the two, but may simply reflect the Galactic radii probed. It is not known empirically how $[\text{O}/\text{Fe}]$ varies in the inner thin disk but models constructed to reproduce the Galactic abundance gradient imply that $[\text{O}/\text{Fe}]$ at a Galactocentric radius of 4 kpc is only ≈ 0.02 dex higher than at the solar location of 8 kpc (Chiappini et al. 2000; Cescutti et al. 2007). This suggests that there should be a significant difference in $[\text{O}/\text{Fe}]$ between the bulge and the thin disk in the transition region in the inner parts of the Galaxy. It remains to be seen whether this conclusion holds also observationally.

We conclude the discussion by briefly arguing why our detected similarities and differences between the populations are robust findings. Since we are primarily interested in studying the relative differences between our bulge, disk and halo samples, the zero-points adopted for our stellar parameters does not matter much, since all stars, regardless of population, have comparable properties determined similarly. Furthermore, both bulge and comparison samples were analysed using the same set of

lines. We believe that not adhering to these principles is the main reason previous studies (e.g. Zoccali et al. 2006; Fulbright et al. 2007; Lecureur et al. 2007) reached different conclusions, by misleadingly comparing their bulge giant results with literature values for main sequence and turn-off disk stars in the solar neighborhood (Bensby et al. 2005; Reddy et al. 2006). Even the particular choice of solar abundances for the normalization of the stellar results in different works can introduce errors as large as the purported abundance differences between the various stellar populations. We circumvent these problems here by adopting a differential analysis of the bulge and disk giants.

4. Concluding remarks

Three obvious follow-up investigations to the present study are urgently needed. The first is to obtain larger samples of bulge and thick-disk giants, especially in the critical metallicity range $-0.5 \leq [\text{Fe}/\text{H}] \leq +0.0$, to confirm that our conclusions regarding the chemical similarities remain unaltered. Secondly, the analysis should be extended to a determination of additional elements; here Mg is particularly desirable, since Fulbright et al. (2007) and Lecureur et al. (2007) argue that it shows pronounced differences of about 0.2 dex between the bulge giants and local thick-disk dwarfs. Finally, one needs to have a comparison sample from the inner disk analysed in a homogeneous way. Do the chemical similarities between the bulge and the thick disk remain when moving from the solar neighborhood to the inner regions of the Galaxy? Is the Galactic abundance gradient sufficient to make the inner thin disk indistinguishable from the bulge? If so, it would argue in favor of a disk instability rather than a merger origin for the bulge. Until the launch of GAIA, it will be difficult to differentiate kinematically between the thin and thick disks at such large distances, but the chemical signatures may be sufficient since Ramírez et al. (2007) have shown that there is no intermediate disk population at $[\text{Fe}/\text{H}] \approx -0.3$, locally. More work is clearly needed to establish the causal relationships, if any, between the bulge and the thin and thick disks in the inner regions of the Galaxy.

Acknowledgements. We thank S. Schuler and K. Hinkle for assisting with carrying out some of the Gemini/Phoenix observations. Based on observations obtained at the Gemini Observatory, which is operated by the AURA, Inc., under a cooperative agreement with the NSF on behalf of the Gemini partnership: the NSF (United States), the STFC (United Kingdom), the NRC (Canada), CONICYT (Chile), the ARC (Australia), CNPq (Brazil) and SECYT (Argentina). This paper uses data obtained with the Phoenix infrared spectrograph, developed and operated by NOAO. This work has been supported by ARC (DP0588836), ANSTO (06/07-0-11) and NSF (AST 06-46790).

References

- Alonso, A., Arribas, S., & Martínez-Roger, C. 1999, *A&AS*, 140, 261
- Asplund, M. 2005, *ARA&A*, 43, 481
- Asplund, M., Grevesse, N., & Sauval, A. J. 2005, in *ASP Conf. Series*, Vol. 336, 25
- Ballero, S. K., Matteucci, F., Origlia, L., & Rich, R. M. 2007, *A&A*, 467, 123
- Bensby, T., Feltzing, S., & Lundström, I. 2004, *A&A*, 415, 155
- Bensby, T., Zenn, A. R., Oey, M. S., & Feltzing, S. 2007, *ApJ*, 663, L13
- Castelli, F., Gratton, R. G., & Kurucz, R. L. 1997, *A&A*, 318, 841
- Cescutti, G., Matteucci, F., François, P., & Chiappini, C. 2007, *A&A*, 462, 943
- Chiappini, C., Matteucci, F., & Padoan, P. 2000, *ApJ*, 528, 711
- Collet, R., Asplund, M., & Trampedach, R. 2007, *A&A*, 469, 687
- Cunha, K. & Smith, V. V. 2006, *ApJ*, 651, 491
- da Silva, L., Girardi, L., Pasquini, L., et al. 2006, *A&A*, 458, 609
- Demarque, P., Woo, J.-H., Kim, Y.-C., & Yi, S. K. 2004, *ApJS*, 155, 667
- Fulbright, J. P., McWilliam, A., & Rich, R. M. 2006, *ApJ*, 636, 821
- Fulbright, J. P., McWilliam, A., & Rich, R. M. 2007, *ApJ*, 661, 1152
- Gratton, R., Sneden, C., & Carretta, E. 2004, *ARA&A*, 42, 385

Gustafsson, B., Edvardsson, B., Eriksson, K., et al. 2003, in ASP Conf. Series, Vol. 288, , 331
Hinkle, K. H., Blum, R. D., Joyce, R. R., et al. 2003, in SPIE, Vol. 4834, , 353
Kormendy, J. & Kennicutt, Jr., R. C. 2004, ARA&A, 42, 603
Lecureur, A., Hill, V., Zoccali, M., et al. 2007, A&A, 465, 799
McWilliam, A. & Rich, R. M. 1994, ApJS, 91, 749
Meléndez, J., Barbuy, B., Bica, E., et al. 2003, A&A, 411, 417
Meléndez, J. & Ramírez, I. 2007, ApJ, 669, L89
Meléndez, J., Shchukina, N. G., Vasiljeva, I. E., & Ramírez, I. 2006, ApJ, 642, 1082
Ramírez, I., Allende Prieto, C., & Lambert, D. L. 2007, A&A, 465, 271
Ramírez, I. & Meléndez, J. 2005, ApJ, 626, 465
Reddy, B. E., Lambert, D. L., & Allende Prieto, C. 2006, MNRAS, 367, 1329
Rich, R. M. & Origlia, L. 2005, ApJ, 634, 1293
Salaris, M., Chieffi, A., & Straniero, O. 1993, ApJ, 414, 580
Snedden, C. A. 1973, PhD thesis, Univ. of Texas, Austin
Stanek, K. Z. 1996, ApJ, 460, L37
Tinsley, B. M. 1980, Fundamentals of Cosmic Physics, 5, 287
van der Kruit, P. C. & Searle, L. 1981, A&A, 95, 105
van Leeuwen, F. 2007, A&A, 474, 653
Yong, D., Aoki, W., Lambert, D. L., & Paulson, D. B. 2006, ApJ, 639, 918
Zoccali, M., Lecureur, A., Barbuy, B., et al. 2006, A&A, 457, L1

Table 1. Stellar parameters and derived abundances

Star	T_{eff}	$\log g$	[Fe/H]	[C/Fe]	[N/Fe]	[O/Fe]
Bulge:						
I012	4237	1.61	-0.43	0.05	0.57	0.42
I025	4370	2.28	0.50	-0.27	0.54	-0.03
I141	4356	1.93	-0.21	0.07	0.49	0.52
I151	4434	1.73	-0.80	0.05	0.31	0.52
I156	4296	1.60	-0.70	-0.04	0.22	0.40
I158	4426	2.68	-0.14	0.12	0.39	0.22
I194	4183	1.67	-0.27	-0.19	0.42	0.36
I202	4252	2.07	0.20	-0.03	0.53	0.12
I264	4046	0.68	-1.16	-0.33	0.89	-0.13
I322	4255	1.90	-0.05	0.04	0.41	0.30
II033	4230	1.37	-0.75	-0.37	0.33	0.39
III152	4143	1.51	-0.46	0.08	0.34	0.41
IV003	4500	1.85	-1.22	-0.17	0.57	0.50
IV072	4276	2.13	0.18	-0.20	0.32	-0.13
IV167	4374	2.44	0.40	-0.24	0.39	-0.10
IV203	3815	0.35	-1.29	-0.58	0.91	0.08
IV325	4353	2.35	0.40	-0.01	0.48	0.19
IV329	4153	1.15	-0.87	-0.25	0.30	0.31
BW96	4050	1.20	0.05	-0.08	0.61	0.20
Halo:						
HD041667	4581	1.80	-1.07	-0.20	0.23	0.38
HD078050	4951	2.54	-0.93	0.14	-0.01	0.24
HD114095	4794	2.68	-0.55	0.11	0.17	0.54
HD206642	4372	1.57	-0.97	-0.13	0.25	0.46
Thick disk:						
HD008724	4577	1.49	-1.69	-0.40	0.43	0.31
HD077236	4427	2.01	-0.57	0.04	0.25	0.57
HD030608	4620	2.39	-0.22	-0.13	0.40	0.20
HD107328	4417	2.01	-0.30	0.11	0.28	0.45
HD023940	4762	2.61	-0.32	-0.08	0.39	0.30
HD032440	3941	1.15	-0.17	-0.25	0.29	-0.01
HD037763	4630	3.15	0.33	-0.07	0.43	0.00
HD040409	4746	3.20	0.10	-0.07	0.31	-0.04
HD077729	4127	1.48	-0.43	0.08	0.27	0.54
HD080811	4900	3.28	-0.37	-0.05	0.31	0.40
HD083212	4480	1.55	-1.43	-0.43	0.33	0.47
HD099978	4678	2.07	-1.00	-0.03	0.03	0.34
HD107773	4891	3.28	-0.31	-0.02	0.32	0.39
HD119971	4093	1.36	-0.61	-0.06	0.31	0.38
HD124897	4280	1.69	-0.52	0.15	0.23	0.45
HD130952	4742	2.53	-0.28	-0.01	0.28	0.32
HD136014	4774	2.52	-0.40	0.03	0.27	0.36
HD145148	4851	3.67	0.19	-0.10	0.28	0.03
HD180928	4092	1.48	-0.42	0.06	0.24	0.45
HD203344	4666	2.53	-0.16	0.02	0.50	0.29
HD219615	4833	2.51	-0.46	0.02	0.29	0.41
Thin disk:						
HD000787	4020	1.36	0.07	-0.24	0.33	0.02
HD005268	4873	2.54	-0.47	-0.04	0.45	0.30
HD005457	4631	2.67	0.03	-0.19	0.31	0.00
HD018884	3731	0.73	0.02	-0.33	0.32	0.02
HD029139	3891	1.20	-0.15	-0.20	0.30	-0.03
HD029503	4616	2.67	0.11	-0.22	0.48	0.05
HD050778	4034	1.40	-0.26	-0.07	0.31	0.19
HD099648	4837	2.24	-0.02	-0.23	0.34	0.01
HD100920	4788	2.58	-0.08	-0.23	0.32	0.02
HD115478	4272	2.00	0.02	-0.08	0.27	0.04
HD116976	4691	2.49	0.11	-0.09	0.31	-0.06
HD117818	4802	2.59	-0.25	-0.16	0.50	0.28
HD128188	4657	2.03	-1.35	-0.12	0.14	0.35
HD132345	4400	2.34	0.29	-0.12	0.44	-0.10
HD142948	4820	2.24	-0.73	-0.24	0.39	0.48
HD171496	4975	2.40	-0.58	0.14	0.22	0.42
HD172223	4471	2.46	0.26	-0.02	0.36	0.01
HD175219	4720	2.44	-0.32	-0.20	0.31	0.06
HD186378	4566	2.42	0.16	-0.09	0.28	-0.05
HD187195	4405	2.36	0.13	-0.06	0.36	-0.06
HD210295	4738	1.88	-1.23	-0.11	0.06	0.49
HD211075	4305	1.76	-0.33	-0.01	0.11	0.14
HD214276	4586	2.55	0.15	0.05	0.28	0.01
HD214376	4586	2.55	0.15	0.05	0.28	0.01